

FLUORESCENCE PHOTOBLEACHING RECOVERY MEASUREMENT OF PROTEIN ABSOLUTE DIFFUSION CONSTANTS[☆]

B. George BARISAS^{*} and Michael D. LEUTHER

*Edward A. Doisy Department of Biochemistry, St. Louis University School of Medicine,
St. Louis, Missouri 63104, USA*

Received 22 March 1979

The technique of fluorescence photobleaching recovery [Axelrod et al., *Biophys. J.* 16 (1976) 1055] has been applied to the measurement of absolute diffusion constants of a number of fluorescein isothiocyanate-labeled proteins. Measured diffusion constants agree to within $\pm 7\%$ of published values for the underivatized proteins. The method has sufficient sensitivity to reveal the concentration dependence at neutral pH of the diffusion constant of α -chymotrypsin. The rapidity with which the labelling and measurements can be performed and the small amount of material required suggest the technique may be useful in rapid characterization of small protein samples. Some developments in optical and electronic systems and in data processing for this technique are discussed.

1. Introduction

Fluorescence photobleaching recovery (FPR)^{‡1} is an optical technique for measuring the diffusion constant or rate of convective flow of fluorescent molecules in free solution or restricted to the plane of a cell or model membrane. A brief pulse of high-intensity laser light irreversibly bleaches the fluorophores at the focus of the beam. The intensity of the beam is then reduced 10^3 – 10^4 fold and the fluorescence excited by the beam is measured with time as diffusion or convection brings unbleached, fluorescent molecules into the area illuminated by the beam. The kinetics of fluorescence recovery yield the diffusion con-

stant or rate of convective flow of the fluorescent species. To date, most applications of FPR have concerned lateral mobility of the various components of cell and model membranes (see for example [1,2]) and these diffusion constants are frequently determined relative to a standard fluorescent species [3]. A less-explored capability of the technique is the measurement of absolute diffusion constants for fluorescently-conjugated macromolecules. The method takes advantage of a simple and rapid small-scale procedure, developed for preparing fluorescent antibodies, to introduce bleachable fluorescent groups onto a protein without otherwise altering its tertiary structure. The FPR diffusion measurements themselves offer the advantages of speed and small sample requirements. We describe here our application of FPR to measuring the diffusion constants of a number of well-characterized proteins. This work has also given us the opportunity to establish better the accuracy which FPR measurements of absolute diffusion constants are capable of achieving and to develop certain optical and electronic systems which support FPR measurements generally.

[☆] This work supported by NSF grant PCM 76-06523 and by a Cottrell grant from Research Corporation.

^{*} Recipient of a Research Career Development Award from the National Institute of Allergy and Infectious Diseases.

^{‡1} Abbreviations used in this paper are: PBS, phosphate-buffered saline (0.14 M sodium chloride, 0.01 M sodium phosphate, pH 7.0); FPR, fluorescence photobleaching recovery; FCS, fluorescence correlation spectroscopy; FITC, fluorescein isothiocyanate; BSA, bovine serum albumin.

2. Materials and methods

2.1. Instrumentation

Our apparatus for fluorescence photobleaching recovery and for the related technique of fluorescence correlation spectroscopy is illustrated in fig. 1. A Newport Research Corporation 5' by 8' Research Series laser table serves as the mounting base for all optical components. The light source is a Coherent Radiation CR-2 2 watt argon ion laser running in the TEM 00 mode with feedback stabilizer. The laser beam is spatially filtered and collimated and then passes through an interferometric beam attenuator. The expanded laser beam is separated by a beam splitter and mirror into two equal intensity parallel components, the undeviated one of which is normally blocked by a Vincent Associates electronic shutter. The other beam passes through Balzers neutral density filters which attenuate its intensity 10^3 – 10^4 fold. It is reflected onto another beam splitter which recombines it with the undeviated beam. This device permits bleaching pulses of 5 ms to 8 s to be produced without movement of any reflective or absorptive

optical elements. Bleaching and interrogation intensities are separately adjustable. Coincidence of the bleaching pulse and interrogation beams can easily be adjusted to within 3 arc s. A portion of the beam is sampled by a beam splitter, the intensity integrated spatially, and this reference signal monitored by a vacuum photodiode. Steering mirrors direct the beam vertically down into a lens of 12.5 cm focal length. Fig. 2 details the optical system. From here the converging beam passes through a hole in a parabolic reflector, the axis of which is horizontal, and comes to a focus coincident with that of the reflector. The laser beam exits through a hole in the bottom of the reflector and is absorbed by a beam stop. A hole in the rear of the parabolic reflector permits a thermostatted 100 μ m path length flow cell to be placed at the foci of the reflector and the laser beam. Fluorescence emitted from this cell is horizontally collimated by the reflector and passes a light stop which masks out stray light entering through the rear hole. A Fresnel lens then refocuses the fluorescence onto an iris diaphragm located at the entrance image plane of a collimated filter monochromator with slots for one chemical and three glass filters. The exit focal plane

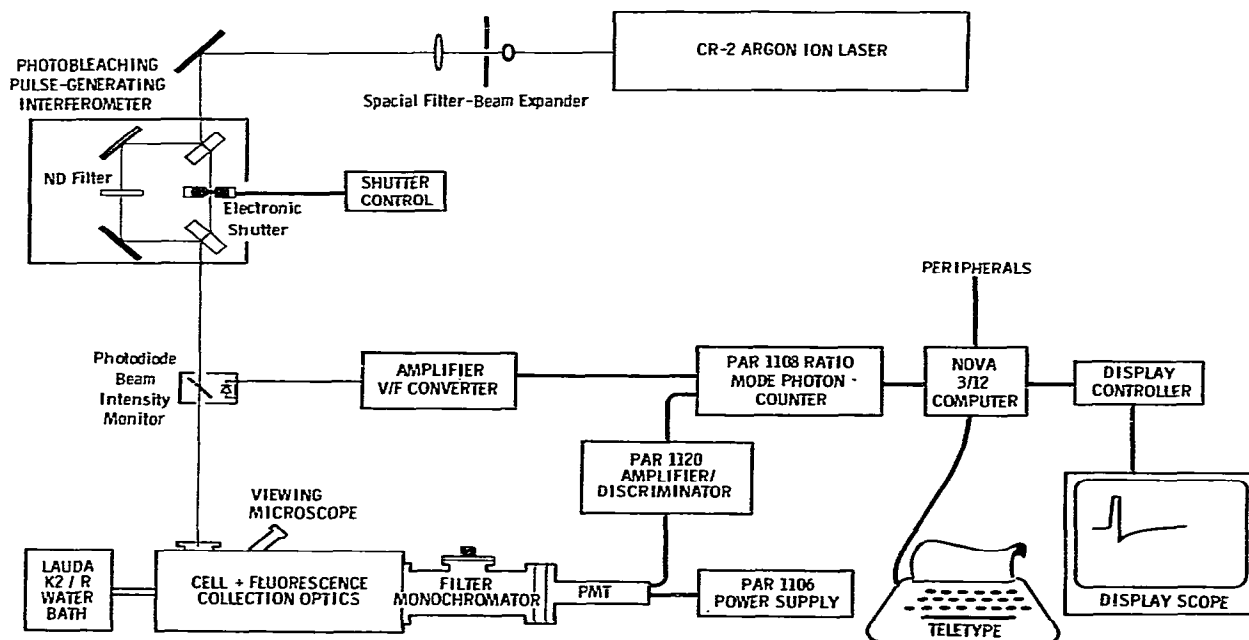


Fig. 1. Schematic diagram of FPR/FCS system. Layout is approximately that of actual device.

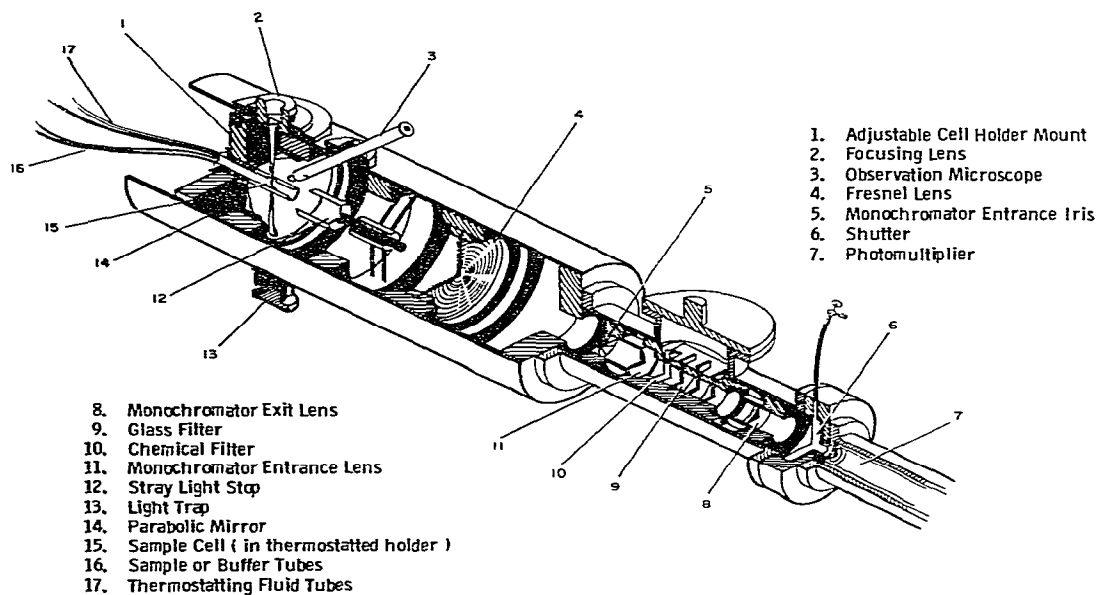


Fig. 2. Detail of FPR/FCS optics tube. The length of the section shown is approximately 90 cm.

of the monochromator coincides with a shutter to protect the photomultiplier which lies immediately behind. A microscope, fittable with assorted barrier filters, sits atop the main optical tube and looks obliquely at the cell. This permits focusing of the laser beam and alignment of the sample cell. The various image stops, stray light barriers, and the use of O-ring seals throughout make this photometer extremely insensitive to ambient illumination. We estimate that close to 35% of the emitted fluorescence is delivered to the photocathode. There are eight refracting surfaces in the optical system (if only the chemical filter is present) and reflections from these surfaces reduce by a factor of 0.75 the 50% of the total fluorescence collimated by the reflector. An RCA 6532 PM tube (S-5 response) provides adequate sensitivity to the large signals observed in these experiments. This optical system is interchangeable with a microscope-based photometer which we use for FPR/FCS studies of viable cells and model membranes [4]. The laser table currently rests on granite mounts and careful axial alignment of the optical system is possible. No vibrational frequencies below 500 Hz have appeared in correlation experiments unless the table was artificially perturbed.

Ratio-mode photon counting has been adopted

to permit, in addition to extraction of maximum information from the emitted photon flux, facile compensation for intensity fluctuations in the exciting laser beam. The compensation for source intensity fluctuations is the pulse counting equivalence of dividing the fluorescence photomultiplier current by a reference photomultiplier current. A Princeton Applied Research model 1108 photon counter is driven by an external clock whose frequency is nominally 1.2 MHz but is proportional to the intensity of the exciting laser beam. The reference channel is preset to the number of counts which would be expected for a 1.0 MHz clock over the appropriate realtime interval. When the reference channel obtains this value after ~83% of the desired counting time interval, the main counter, monitoring fluorescence photons, is shut down until the end of the time period and then both counters are reset at the appropriate realtime point. Thus, the number of counts accumulated in the main channel per time increment is directly proportional to the true ratio of fluorescence intensity to excitation intensity. One modification of the photon counter is the realtime reset feature. The 1108 normally resets only on command of the reference counter which here counts a variable frequency clock and thus would output data at irregular intervals. The

second modification involves replacing the 1108's binary coded decimal (BCD) counters and light emitting diodes (LED) with hexadecimal counters and LED's. This permits direct parallel binary output to the computer, thus, avoiding time-consuming BCD-to-binary conversions.

An amplifier-voltage to frequency converter transforms the laser intensity reference signal from a 1P28 photomultiplier wired as a photodiode into a nominal 1.2 MHz emitter coupled logic level signal. This is fed to the 1108 external clock input for the ratio counting described above. A variable gain control on the amplifier affords a nominal 6 V output which drives a Philbrick 4705 voltage to frequency module to 0.6 MHz output. Frequency doubling affords the desired 1.2 MHz signal. The performance of the complete ratio mode optical/electronic system is outstanding. Modulating the laser via its power supply at 250 Hz and monitoring the resulting fluorescence fluctuations at the photon counter suggest that ~50 fold attenuation of source fluctuations is achieved at this frequency.

The photon counter normally communicates with the NOVA 3/12 computer via a program interrupt. Our data acquisition and processing programs for FPR experiments are written in the BASIC language with interrupt handlers and special functions such as time autocorrelation function calculations residing as machine language subroutines. When the program is idling, the photon counter feeds fluorescence intensities continuously into a circular buffer. When a bleaching pulse is detected, only a fixed number of additional points are recorded and this number is less than the buffer capacity. Thus, points prior to the bleach are saved so that the pre-bleach level is known. The raw data is displayed on the oscilloscope and then additionally processed on line to yield the diffusion constant as described in the next section.

2.2. Data analysis

A detailed treatment of the kinetics of fluorescence recovery after photobleaching has been published by Axelrod et al. [5]. These authors consider both gaussian and uniform circular beam profiles and both diffusive and convective fluorescence recovery. In the gaussian case, the half-time $t_{1/2}$ for diffusive recovery of a photobleaching-induced concentration

fluctuation is given by

$$t_{1/2} = \gamma r^2 / 4D, \quad (1)$$

where r is the $1/e^2$ radius of the laser beam and D is the diffusion constant of the fluorescent species. γ is a parameter dependent upon the degree of photobleaching as measured by a second parameter K (see Axelrod et al. [5]). In our experiments, we chose to restrict K to values of about 0.2. Since, for small K , $\gamma = 1 + (2/21)K + \dots$, we may with very little error set γ equal to one. Moreover, for such small K , a fluorescence fluctuation decays as $1/(1 + t/t_{1/2})$ and we were able to use a linear regression based on this simple time dependence to evaluate $t_{1/2}$.

When the laser beam is focused a distance l behind or ahead of the cell center, the light illuminating the cell still has a gaussian profile [6] with r given by

$$r^2 = r_0^2 [1 + (\lambda/\pi r_0^2)^2], \quad (2)$$

where λ is the wavelength and r_0 is the image $1/e^2$ radius at focus. r_0 is in turn equal to $\lambda f/\pi R_0$ where f is the focusing lens focal length and R_0 is the collimated beam $1/e^2$ radius. Increasing r by this method to ~80 μm permitted easy superimposition of bleaching and interrogation beams in the cell and increased fluorescence recovery times to the convenient time-scale of seconds. f was verified by direct measurement and R_0 was determined by the usual procedure of translating a pinhole across the expanded laser beam [7].

The data acquisition program acquires and displays raw data, evaluates $t_{1/2}$ by the previously mentioned regression, and evaluates D from a knowledge of $t_{1/2}$ and r^2 . Error estimates on diffusion constants are the standard errors of a set of replicate measurements, usually 10 per protein.

2.3. Reagents

Proteins were obtained from standard commercial sources (Sigma, Worthington) and were used without further purification. Fluorescein isothiocyanate (FITC) 10% on Celite was obtained from Calbiochem. FITC-labeled proteins were prepared by the method of Rinderknecht [8] and were equilibrated with PBS and separated from free fluorescein by gel filtration over appropriate porosities of Sephadex or Bio-Gel. Num-

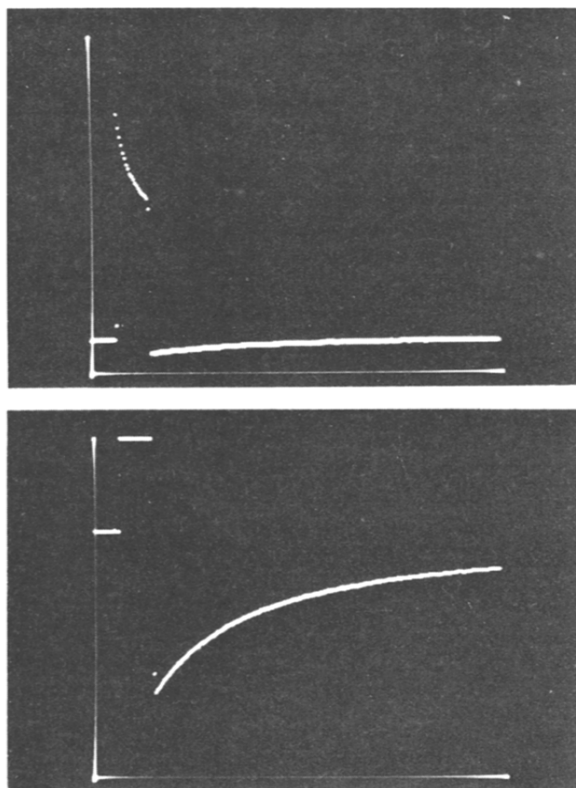


Fig. 3. Fluorescence photobleaching recovery raw data for FITC-bovine serum albumin 0.5 mg/ml in phosphate buffered saline pH 7.0 at 20°, various parameters exaggerated to illustrate bleaching pulse. Excitation 488 nm at 30 μ m radius, 0.5 mW for 1 sec to bleach, 0.05 mW elsewhere. Fluorescence in arbitrary units lies along the vertical axis while the horizontal axis indicates time, full scale being 25 s. Upper trace accentuates the bleaching effect while the lower trace shows the fluorescence recovery. Implied diffusion constant is $7.1 \times 10^{-7} \text{ cm}^2 \text{ s}^{-1}$.

bers of fluorescein molecules bound per protein molecule ranged from 1×10^{-3} to 7×10^{-2} and were determined by optical density measurements [9] at 280 and 496 nm assuming molar extinction coefficients for fluorescein at these wavelengths of 21 500 cm^{-1} and 59 800 cm^{-1} , respectively. In no case did the degree of labeling even approach one mole of fluorescein per mole of oligomer. Thus, diffusion measurements were made on relatively well-defined molecular species, namely proteins bearing only a single, randomly-located fluorescein per oligomer.

2.4. Experimental conditions

Measurements were made at a temperature of $20 \pm 0.3^\circ\text{C}$ on protein conjugate solutions usually 0.5 mg ml^{-1} . Excitation of FITC fluorescence was via either the 488 nm or the 514 nm Ar lines using a power of $\sim 25 \text{ mW}$ for 1/2 – 1 second for bleaching and 25 μW for monitoring fluorescence recovery. The chemical barrier filter consisted of a 1 cm pathlength of saturated aqueous potassium dichromate. $1/e^2$ radii of the bleaching and interrogation beams were $\sim 80 \mu\text{m}$.

3. Results and discussion

The raw data obtained in these experiments is illustrated by fig. 3 which shows photobleaching recovery kinetics for FITC-BSA. The upper trace shows the approximately exponential falloff in fluorescence intensity during the bleaching pulse and the correspondingly reduced fluorescence observed after the laser beam intensity returns to its original low level. To illustrate both these features on a single trace, the ratio of the bleaching to interrogation beam intensities had to be restricted to 10 : 1 instead of the usual 10^3 – 10^4 : 1. The lower trace details the recovery kinetics for the above bleaching pulse. While the extent of bleaching ($K \approx 1$) is too large for simple $1/(1 + t/t_{1/2})$ recovery kinetics to be obeyed, the main feature of these kinetics is apparent, namely a much slower return to the pre-bleach fluorescence level than would be expected for the exponential they superficially resemble.

The use of a simple linear regression to extract the recovery half-time is illustrated in fig. 4 for FITC-conjugated bovine serum albumin. Here the reciprocal fractional fluorescence reduction $\langle F \rangle / \Delta F$ is plotted versus time as is normally performed on-line by the data acquisition program. Although K was 0.34, rather larger than was normally used, the limiting expression for small K fits the data well. A value of γ equal to 1.032 would permit accurate calculation of the diffusion coefficient using eq. (1) from the recovery half-time. This general procedure points the way for rapid on-line processing of FPR data, even when large values of K are encountered. The raw data are fitted by a polynomial of an appropriate number of terms in

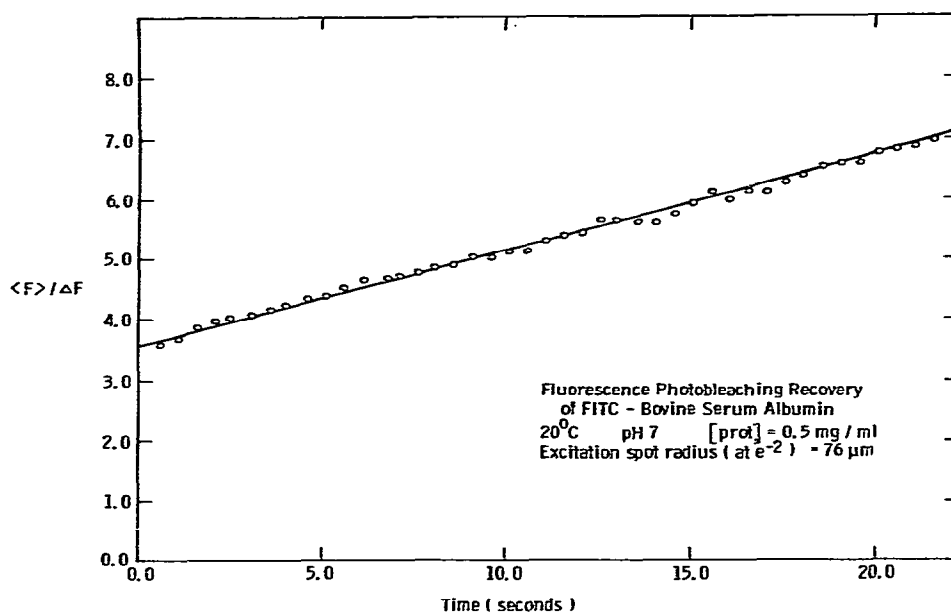


Fig. 4. Plot to determine half-time for fluorescence recovery of mobile fluorophores. Sample is FITC-bovine serum albumin 0.5 mg/ml in phosphate-buffered saline pH 7.0 at 20°C. Excitation 488 nm at 76 μm radius, 50 mW for 1 s to bleach, 0.05 mW elsewhere. For this example, $k = 0.34$, slope and intercept of fitted curve yield $t_{1/2} = 22.19$ s.

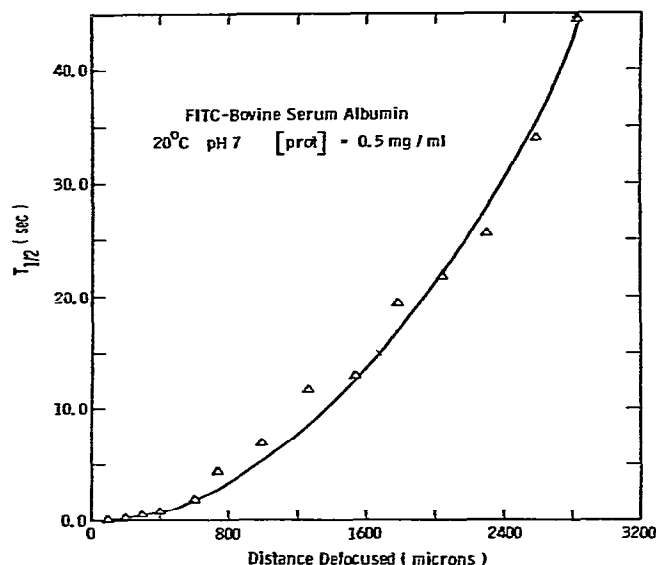


Fig. 5. Plot of FPR half-time versus distance from cell center to beam image plane. FITC-bovine serum albumin 0.5 mg/ml in PBS, pH 7.0, 20°. Excitation 488 nm, 50 mW to bleach, 0.05 mW otherwise. $K \sim 0.2$. Spot radius at focus 4.01 μm . Smooth curve results from calculating first the radius for the out-of-focus spot and then $t_{1/2}$ assuming a diffusion constant of $6.8 \times 10^{-7} \text{ cm}^2 \text{ s}^{-1}$.

$\langle F \rangle / \Delta F$ and the results used to precisely determine K and $t_{1/2}$. The value of γ appropriate to K can be selected and the diffusion constant calculated. This method is superior to the graphical technique of Axelrod and co-workers [5] in that it is easily implemented by computer and uses all the available data in the regression which eventually determines $t_{1/2}$. This data processing program, suitably modified to evaluate the fraction of immobile fluorescent species encountered on cell surfaces, has worked especially well in our studies of lymphocyte stimulation [4].

The experimental dependence of fluorescence recovery half-time on the distance from cell center to the beam image plane is shown in fig. 5. The smooth curve results from calculating first the radius of the out-of-focus spot and then $t_{1/2}$ assuming for bovine serum albumin the published diffusion constant of $6.8 \times 10^{-7} \text{ cm}^2 \text{ s}^{-1}$. Our measurements are made with the beam focus approximately 2 mm from cell center and we estimate that we can reproduce this distance to an accuracy of ± 0.04 mm between runs. Because of the quadratic dependence of $t_{1/2}$ on l , this implies a $\pm 4\%$ uncertainty in measured values of $t_{1/2}$ and, hence, in D .

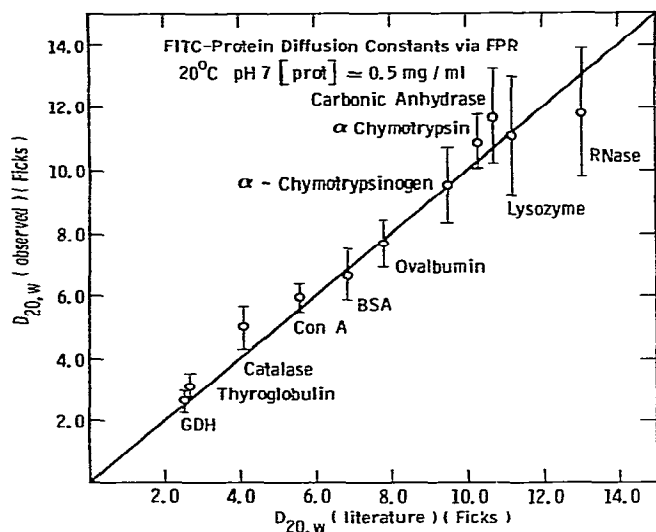


Fig. 6. Diffusion constants for FITC-proteins obtained via FPR compared with literature values for underivatized proteins. Excitation 488 nm at 76 μm radius, 50 mW for 1/4 s to bleach, 0.5 mW otherwise. $K \sim 0.2$. Proteins 0.5 mg/ml in PBS, pH 7.0, 20°C. Sources of published data on protein diffusion constants are: glutamate dehydrogenase, [14]; catalase [15]; α -chymotrypsin [16]; carbonic anhydrase [17]; lysozyme [18]; ribonuclease [19]; α -chymotrypsinogen [20]; thyroglobulin [21]; bovine serum albumin [22]; ovalbumin [23]; concanavalin A [24].

In fig. 6, diffusion constants obtained via FPR for FITC-labeled proteins are compared with literature values for underivatized proteins. The details of these determinations are given in the caption of this figure as are sources of the literature values of $D_{20,w}$. No effort has been made to extrapolate these particular results to zero protein concentrations. The measured diffusion constants for the protein conjugates agree with literature values for underivatized proteins to an average extent of $\pm 7\%$. The main sources of random errors in these determinations would seem to be superimposition for bleaching and interrogation beams (as will be discussed later) and accuracy of displacing the cell relative to the beam focus. The probable magnitudes of these uncertainties in our experimental situation lead by propagation of error methods to about a 6% uncertainty in measured values of D . This probably approximates the absolute limit of accuracy of FPR diffusion constant determinations. The major source

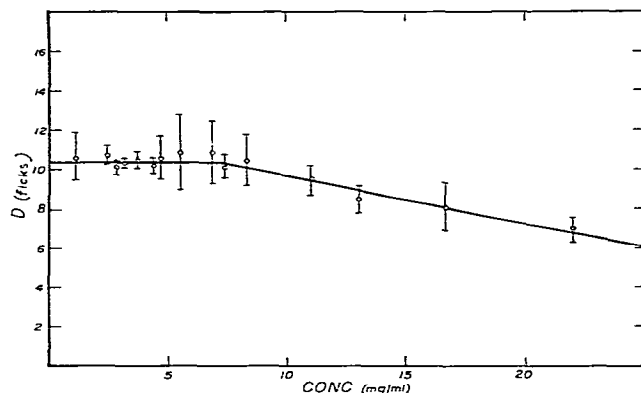


Fig. 7. Concentration dependence of measured diffusion constant of α -chymotrypsin. Solutions in PBS, ionic strength 0.16 M, pH 7.0, 20°C. Excitation 514 nm at 80 μm 1/e² radius, 50 mW for 1 sec to bleach, 50 μW otherwise.

of systematic error is uncertainty in the value of r_0^2 . We feel we can measure the expanded beam radius to $\pm 4\%$ and the focal length of the focusing lens to $\pm 2\%$. These values imply a $\pm 10\%$ uncertainty in r_0^2 and, hence, in measured values of D . On the other hand, all measurements made using a given optical system will be equally affected by an incorrect value of r_0^2 . Therefore, errors from this source can, in theory, be corrected by calibration against materials of known diffusion constant. Without such calibration, this systematic error, combined with the random errors mentioned above, limited the accuracy of absolute diffusion constant measurements to $\pm 12\%$.

The concentration dependence of the diffusion constant of α -chymotrypsin is shown in fig. 7. Under the experimental conditions (pH 7 and ionic strength of 0.16 M), α -chymotrypsin associates to form not only dimers but also high oligomer [10]. The diffusion constant at high protein concentrations, therefore, does not stabilize at the value of 8.36 Ficks to be expected for the dimer^{‡2} [11], but continues to decrease with increasing protein concentration.

Pandit and Rao [10] have studied the self-associ-

^{‡2} The diffusion constant for the dimer can be estimated from the sedimentation coefficients of 4.1 s and 2.5 s measured by Aune et al. (1971) for the monomer and dimer, respectively, by assuming that the partial specific volumes of both species are approximately equal.

tion of α -chymotrypsin at pH 6.9 and ionic strength of 0.10 M. Under these conditions which closely approximate ours, they observe a weight-average molecular weight corresponding to dimer at a protein concentration of about 12 mg/ml. Our value of D corresponding to dimer occurs at a protein concentration of about 15 mg/ml so, to a first approximation, we seem to observe the same concentration dependence of hydrodynamic properties observed in the ultracentrifuge for unmodified chymotrypsin.

Several factors contribute to the ability of this technique to determine absolute diffusion constants with good accuracy. The first of these is the accurately known beam profile at the cell. We have closed the exit iris of our laser down somewhat, sacrificing output power to reduce TEM₀₁ mode content, interposed a spacial filter, and, finally, measured the gaussian profile of the resulting collimated beam by the usual procedure of translating a pinhole across its diameter. Since the beam has a radius of about 0.43 cm and the focusing lens a radius of 1.25 cm, there is no significant diffraction from the lens aperture in the image plane. Moreover, these measurements were performed with the cell located about 2 mm from the beam focus. In such a case any aberrations of the lens have little to do with the image profile at the cell. The shortness of the cell's 100 μ m path length relative to the 12.5 cm focal length of the focusing lens means that the beam radius at the cell varies only $\pm 2 \mu$ m from the front to the rear of the cell. This insures that the effect of diffusion parallel to the beam axis on the measured signal is minimal.

Probably the most important factor in making accurate or even reproducible measurements of diffusion constants by FPR is using an interferometric pulse generator to avoid moving neutral filters in and out of the beam path. If accurate values of diffusion constants are to be measured by FPR, there must be excellent superimposition on the sample of the bleaching pulse and the interrogation beam. Especially when measurements are made with focused beams, as happens in microscope-based studies of bilayers or cell membrane, this is difficult to achieve. Any wedge in the filter will displace the interrogation beam relative to the bleaching beam and yield artificially long recovery times. High optical quality filter substrates have a wedge specification of 5 minutes of arc. On the other hand, it can be shown (Barisas, in preparation)

that to obtain, with focused beams, $t_{1/2}$ values accurate to -0% , $+10\%$, the bleaching and interrogation beams can deviate by a maximum of 15 arc s. Even with careful selection of filters, it is difficult to achieve this low a wedge. Moreover, if the filter has local variations in flatness, any lack of reproducibility in positioning the filter will yield irreproducible values of recovery time.

Our results demonstrate that the absolute diffusion constants of fluorescently-conjugated proteins can be measured rapidly and with good accuracy using the techniques of fluorescence photobleaching recovery. The major uncertainty connected with the application of this technique is what effect the FITC-conjugation has on the hydrodynamic properties of the proteins being examined. A complete answer to this question would require immunochemical or isoelectric focusing isolation of protein molecules bearing single fluorescein groups and characterization of these conjugates by ultracentrifuge. On the other hand the results shown in figs. 6 and 7 lead one to the empirical conclusion that measuring the diffusion constants of protein conjugates gives good estimates of the diffusion constants of the underivatized proteins. The rapidity with which the labeling and the measurements can be performed and the small amount of material required suggest the technique might be useful in rapid characterization of small protein samples. Also, if protein conjugates were examined in the presence of sodium dodecyl sulfate and β -mercaptoethanol, the peptides, existing as extended, highly asymmetric structures, should exhibit diffusion constants with strong inverse dependence on their molecular weights. This would afford a rapid method of peptide molecular weight determination precisely analogous to the polyacrylamide gel electrophoretic technique of Weber and Osborn [12].

Perhaps the greater inherent limitation of this method is the difficulty of studying heterogeneous macromolecular systems. If two components of a mixture differ in their diffusion constants by, say, a factor of ten, then manual evaluation of the separate diffusion constants should present no problem. If, on the other hand, the diffusion constants are similar, some unbiased method of resolving kinetic data into components attributable to single diffusion constants must be found. A method of moments analogous to that of Isenberg and Dyson [13] could probably be devised; but, because a single component recovers in time slowly as

$1/(1 + t/t_{1/2})$ instead of as rapidly as an exponential, the cut-off correction is likely to be a problem of major magnitude. Alternatively, the bleaching and interrogation beam geometries might be altered to give exponential recovery kinetics so that Isenberg and Dyson's [13] method could be applied directly. Even if a good method for resolving kinetic data is available, the actual amounts of species possessing various diffusion constants can never be determined by this technique. The amount of fluorescent label which any given protein takes up under the conditions used for conjugation will vary greatly from protein to protein and cannot be predicted in advance. Thus the technique would be most useful for homogeneous biopolymers, with possible limited applicability to estimating the diffusion constants exhibited by major components of a heterogenous sample.

References

- [1] D. Axelrod, A. Wight, W.W. Webb and A. Horwitz, *Biochemistry* 17 (1978) 3604.
- [2] P.F. Fahey and W.W. Webb, *Biochemistry* 17 (1978) 3046.
- [3] D.E. Wolf, J. Schlessinger, E.L. Elson, W.W. Webb, R. Blumenthal and P. Henkart, *Biochemistry* 16 (1977) 3476.
- [4] J.S. Peacock, M.D. Leuther, H. Krakauer and B.G. Barisas, *Biophysical J.* 25 (1979) 168a.
- [5] D. Axelrod, D.E. Koppel, J. Schlessinger, E. Elson and W.W. Webb, *Biophysical J.* 16 (1976) 1055.
- [6] H. Kogelnik and T. Li, *Applied Optics* 5 (1966) 1550.
- [7] D. Magde, E.L. Elson and W.W. Webb, *Biopolymers* 13 (1974) 29.
- [8] H. Rinderknecht, *Nature* 193 (1962) 167.
- [9] M. Goldman, *Fluorescent antibody methods* (Academic Press, New York, 1968).
- [10] M.W. Pandit and M.S.N. Rao, *Biochemistry* 15 (1975) 4106.
- [11] K.C. Aune, L.C. Goldsmith and S.N. Timasheff, *Biochemistry* 10 (1971) 1517.
- [12] K. Weber and M. Osborn, *J. Biol. Chem.* 244 (1969) 4406.
- [13] I. Isenberg and R.D. Dyson, *Biophys. J.* 9 (1969) 1337.
- [14] J.A. Olsen and C.B. Anfinsen, *J. Biol. Chem.* 197 (1952) 67.
- [15] J.B. Sumner and N. Gralin, *J. Biol. Chem.* 125 (1938) 33.
- [16] G.W. Schwert and S. Kaufman, *J. Biol. Chem.* 190 (1951) 807.
- [17] M.L. Petermann and N.V. Hakala, *J. Biol. Chem.* 145 (1942) 701.
- [18] A.J. Sophranopoulos, C.K. Rhodes, D.N. Holcomb and K.E. Van Holde, *J. Biol. Chem.* 237 (1962) 1107.
- [19] A. Rothen, *J. Gen. Physiology* 24 (1940) 203.
- [20] P.E. Wilcox, J. Kraut, R.D. Wade and H. Neurath, *Biochimica et Biophysica Acta* 24 (1975) 72.
- [21] Y. Durien, R. Michel, K.O. Pedersen and L. Roche, *Biochimica et Biophysica Acta* 3 (1949) 436.
- [22] J.M. Creeth, *Biochemical J.* 51 (1952) 10.
- [23] O. Lamm and A. Polson, *Biochemical J.* 30 (1936) 528.
- [24] J.B. Sumner, N. Grates and Inga-Brutta Eriksson-Quensel, *J. Biol. Chem.* 125 (1938) 45.